Silica nanoparticles induced the pre-thrombotic state in rats via activation of coagulation factor XII and JNK- NF-κB/AP-1 pathway

Journal:	*Toxicology Research*
Manuscript ID	TX-REV-04-2015-000118.R1
Article Type:	Paper
Date Submitted by the Author:	03-Sep-2015
Complete List of Authors:	Jiang, Lizhen; Capital Medical University, Li, Yanbo; Capital Medical University, ; Beijing Key Laboratory of Environmental Toxicology, Li, Yang; Capital Medical University, ; Beijing Key Laboratory of Environmental Toxicology, Guo, Caixia; Capital Medical University, ; Beijing Key Laboratory of Environmental Toxicology, Capital Medical University, Yu, Yongbo; Capital Medical University, Zou, Yang; Capital Medical University, ; Novartis Institute For Tropical Diseases, Beijing Friendship Hospital, Capital Medical University, Yang, Yumei; Capital Medical University, ; Beijing Key Laboratory of Environmental Toxicology, Capital Medical University, Yu, Yang; Capital Medical University, ; Beijing Key Laboratory of Environmental Toxicology, Capital Medical University, Duan, Junchao; Capital Medical University, ; Beijing Key Laboratory of Environmental Toxicology, Capital Medical University, Geng, Weijia; Capital Medical University, Li, Qiuling; Capital Medical University, Sun, Zhiwei; Capital Medical University, ; Beijing Key Laboratory of Environmental Toxicology, Capital Medical University,

SCHOLARONE™
Manuscripts

Silica nanoparticles induced the pre-thrombotic state in rats via activation of coagulation factor XII and JNK-NF-κB/AP-1 pathway

Lizhen Jiang[1], Yanbo Li[1,2], Yang Li[1,2], Caixia Guo[1,2], Yongbo Yu[1], Yang Zou[1,3], Yumei Yang[1,2], Yang Yu[1,2], Junchao Duan[1,2], Weijia Geng[1], Qiuling Li[1], Zhiwei Sun[*,1,2]

[1] *School of Public Health, Capital Medical University, Beijing, 100069, P.R. China*

[2] *Beijing Key Laboratory of Environmental Toxicology, Capital Medical University, Beijing, 100069, P.R. China*

[3] *Novartis Institute For Tropical Diseases, Beijing Friendship Hospital, Capital Medical University, 100050, P. R. China*

*Corresponding author: Zhiwei Sun, School of Public Health, Capital Medical University, Beijing, 100069, P.R. China. Tel: +86 010 83911507; Fax: +86 010 83911507.

Abstract

Silica nanoparticles (SiNPs) play a vital role in medical applications such as drug delivery and cancer therapy. SiNPs can translocate into bloodstream through all possible routes of entry. However, there is scarce study on pre-thrombotic effect of SiNPs and mechanism of pre-thrombotic state *in vivo*. We specifically focused on the changes of platelets function and blood coagulation in Wistar rats after consecutive 7 days' intravenous injection of SiNPs (52 nm). The platelets aggregation assay, structural changes of platelets membrane glucoproteins, coagulation test, coagulant/anti-coagulant and fibrinolytic factors and the possible molecular mechanism of pre-thrombotic state formation were performed. Our results demonstrated a significant increase in platelets aggregation rate and platelet activation after SiNPs exposure. Clotting time was significantly shortened while fibrinogen (FIB) contents were increased. There were sustained increases in coagulation factors and thrombin-antithrombin complex (TAT) expression induced by SiNPs. Antithrombin III (AT-III) of the SiNPs-treated groups were significantly decreased while concentrations of tissue factor pathway inhibitor (TFPI), tissue plasminogen activator (t-PA) and D-dimer were elevated. The phosphorylation of nuclear factor-κB/p65 (NF-κB/p65) and activator protein-1/c-Jun (AP-1/c-Jun) and the protein levels of JNK were increased after SiNPs exposure. In summary, our results supported that SiNPs induced the hypercoagulable and pre-thrombotic state in rats through the interaction between platelets activation, coagulation system hyperfunction, anti-coagulation and fibrinolytic resistance. Direct interaction between SiNPs and coagulation factor XII (F XII) and JNK- NF-κB/AP-1 pathway might be involved in regulation of pre-thrombotic state formation.

2

Introduction

Nowadays, plenty of novel and advanced nanomaterials (having at least one spatial dimension in the size range 1-100 nm) have been created and extensively applied with the rapid development of nanotechnology. Silica nanoparticles (SiNPs), as the most widely used nanomaterial, are proven to provide certain benefits in various fields of industry (semiconductor, printer toner), consume products (cosmetics, food additives) and biomedicine, especially in medical applications such as DNA delivery, imaging, drug delivery and cancer therapy.[1,2] With the promising application of SiNPs in nanomedicine, intravenous administration becomes a common and important iatrogenic route.[3] In addition, SiNPs can translocate into bloodstream through all possible routes of entry, including inhalation exposure, oral ingestion and dermal absorption.[4,5] Epidemiologic studies revealed that a 1.0% increase in daily mortality had been related to the short-term elevation of particulate matter < 2.5 nm in aerodynamic diameter ($PM_{2.5}$), and the cardiovascular disease was treated as the absolute risk for mortality to PM exposure.[6] An investigation of a group of steel workers in Italy showed that inhalation of PM could induce coagulation disorder that prothrombin time (PT) was significantly shortened, and PM exposure levels were associated with thrombin generation and tissue plasminogen activator (t-PA) elevation, indicating that PM might enhance the blood coagulation.[7] It is well known that nanoparticles (NPs) dominate 99% of

particles numbers in PM, the biocompatibility and hematotoxicity of NPs should be carefully

evaluated.

However, limited studies on the blood coagulation of NPs *in vivo* are performed. There

are initial toxicological studies demonstrated that acute exposure to quantum dots (QD) can

induce some pre-thrombotic effects, and the carboxyl-QDs had more potential to cause

pulmonary vascular thrombosis than the amine-QDs.[8] Sliver NPs enhanced platelets

aggregation in human washed platelets and induced P-selectin release and thrombus

formation in rats.[9] Multi-walled carbon nanotubes (MCWNT), single wall carbon nanotubes

(SCWNT) and SiNPs could also induce potent pro-coagulant activities in the pulmonary

circulation or microcirculation.[10-12] Whereas, contrary to the conclusions that SiNPs could

induce the hypercoagulation and thrombotic diseases, Tokuyuki Yoshida et al found that the

bleeding time and activated partial thromboplastin time (APTT) were prolonged by SiNPs (30

nm and 70 nm) in BALB/c mice, giving evidences that hypocoagulant state and hemorrhagic

tendency were induced by SiNPs,[13] these contradictory results suggest that effects and

mechanism of SiNPs on the blood coagulation need further investigation.

We have previously found that intratracheal instillation of SiNPs with different sizes

can cause endothelial dysfunction, coagulation disorder and cardiovascular toxicity through

inflammatory reaction and oxidative stress,[14] which is consistent with other studies.[1,15,16] Our

recent study concluded that SiNPs could induce endothelial cells dysfunction via oxidative

stress and apoptosis.[17] Meanwhile, tiny homogeneity fibrin thrombi by Martius Scarlet Blue

(MSB) staining had been discovered in the lung sections of dead mice in acute toxicity study

of amorphous SiNPs, thus we hypothesized that SiNPs might promote disseminated

intravascular coagulation (DIC) to generate, followed by wide microthrombus formation, multiple organ failure and even death.[18] However, we still barely have knowledge about the effects of SiNPs on the facilitation of pre-thrombotic state and the destruction of blood homeostasis, let alone the possible mechanism involved in the activation of coagulation factors. Besides, coagulation is a complicated event, it depends on the interaction between pro- and anti-coagulant components, involving vascular constriction, endothelial damage, platelets activation, coagulation factor release and fibrin formation.[19,20] Although the association between SiNPs and platelets activation and coagulation system have been mentioned, there are scarce studies on the effects of SiNPs on anti-coagulation and fibrinolytic system to maintain the circulation homeostasis. Additionally, our preliminary experiment found that the blood coagulation parameter changed over time, we wondered if the process of pre-thrombotic state to thrombus formation is reversible. We specifically designed this experiment to focus on the systemic performances of pre-thrombotic state caused by SiNPs via interaction between platelets activation, coagulation cascade initiation, anti-coagulation and fibrinolytic resistance. Moreover, the potential regulated mechanism and signaling pathway of pre-thrombotic state formation *in vivo* were first discussed in this study. It will provide scientific basis for understanding the cardiovascular effects of SiNPs and meet the urgent need for risk evaluation of SiNPs in medical applications.

Materials and Methods

Characterization of silica nanoparticles

The amorphous SiNPs were prepared using Stöber method[21] by the school of Chemistry, Jilin University, China. The particles were isolated by centrifugation (12,000 rpm/min,

15min), washed three times with saline solution, and then dispersed in 50 mL of sterile saline

solution (making final mass concentration at 13 g/L). The morphology characteristics and size

distribution of SiNPs were determined by transmission electron microscope (TEM) (JEOL,

Japan). A Zeta electric potential granulometer (Malvern Nano-ZS90, UK) was employed to

measure the Zeta potential and hydrodynamic sizes of SiNPs in saline solution at the

concentrations of 500, 250, 125 μg/mL. The SiNPs suspensions were sonicated for 5 min

through a sonicator (160 W, 20 kHz, 5 min; Bioruptor UDC-200, Belgium) before addition to

the dispersion medium to minimize their aggregation and prepared in triplicate for each

concentration. The purity of SiNPs was evaluated by ICP-OES (Thermo Fisher Scientific,

Switzerland).[18] Gel clot Limulus Amebocyte Lysate (LAL) assay was performed to detect the

endotoxin in SiNPs suspensions at concentrations of 0.75, 1.5, 3, 6, and 12 mg/mL. The gel

clot LAL reagents were purchased from Bokang Marine Biological Company, LTD (Zhan

Jiang, China), including endotoxin standard, LAL water, and tachypleus amebocyte lysate

(TAL), whose sensitivity(λ) was 0.125 EU/ml.

Experiment design

Male Wistar rats (180-220 g) were purchased from Weitong-Lihua Experimental

Animal Center (Beijing, China). The animals were raised in plastic cages with stainless steel

mesh lids in a ventilated room (20 ± 2 °C, 50–70% relative humidity, with a 12h light/dark

cycle). Water and food for maintenance were provided ad libitum for a week. All animal care

and experimentations were approved by the Animal Ethics Committee at Capital Medical

University (approval number 2013-X-68).

After one week accommodation, rats were randomly divided to control groups and experiment groups for eight rats each. 52 nm SiNPs saline suspensions were intravenously injected to the experiment group rats via the tail vein with 20 mg/Kg concentration for consecutive 7 days, while the control groups were given with 0.9% saline. At day1, 3 and 7 post exposure, rats were anesthetized with 3.5% chloral hydrate (Figure 1). Blood samples were collected from abdominal aorta into tubes with sodium citrate and EDTA (Becton and Dickinson Company, UK) respectively. The plasma and serum were stored in -80°C until analysis.

Hematology analysis

Blood samples were collected to tubes with ethylene diamine tetraacetic acid (EDTA) at the 1th, 3th and 7th day of intravenous injection to SiNPs for consecutive 7 days. Whole blood samples were analyzed with Veterinary Blood Analyzer (Mindray, China) to determine the number of platelets in whole blood of Wistar rats.

Coagulation parameters test

Blood samples were collected into tubes with sodium citrate at the 1th, 3th and 7th day of intravenous injection to SiNPs for consecutive 7 days. APTT, PT, thrombin time (TT) and FIB were examined by ACL9000 automatic coagulometer (Beckman Coulter, USA).

Platelets aggregation assay

Whole blood samples collected in tubes with sodium citrate were centrifuged at 800 rpm for 10 min and platelets-rich plasma (PRP) was obtained. Some of PRP were centrifuged at 2000 rpm for 5 min, and platelets-poor plasma (PPP) was collected. Platelets aggregation induced by Adenosine diphosphate (ADP) (10.0 μmol/L) (LBY-NJ4, Precil, China) was

measured using Semi-automatic Platelet Aggregometer (LBY-NJ4, Precil, China). Maximum

platelet aggregation rates were generally selected for analysis.

Measurement of CD42d and CD61 activity

The PRP were centrifuged at 2000 rpm for 10 min, washed platelets were resuspended

in phosphate buffered saline (PBS) at 1×10^7 platelets/ml concentration. Flow cytometry was

performed using a special order BD-SRFortessa (Becton and Dickinson Company, UK) on

single stained platelet suspensions as already made. To analyze the function of platelets,

platelet suspensions mixed with fluorescein isothiocyanate (FITC) Anti-Rat CD42d

(anti-GPV) and phycoerythrin (PE) Anti-Rat CD61 (anti- GPIIIa) (Becton and Dickinson

Company, UK) were incubated in the dark at room temperature for 15 min. Then 10,000

platelet-specific events were analyzed by the cytometer for fluorescence.

Histopathological examination

The heart, liver, spleen, lung and kidney were removed and fixed in 10% formalin,

embedded in paraffin, and sectioned. The lung sections were stained with hematoxylin and

eosin (HE) for histological examination according to standard techniques. After staining, the

slides were observed and examined by optical microscope (Olympus X71-F22PH, Japan).

The fields were chosen randomly and continuously.

Immunohistochemistry

Tissue factor (TF) was detected immunohistochemically in the paraffin embedded lung

sections. After the deparaffination and rehydration of sections, EDTA buffer (pH 9.0)

was added for the antigen retrieval in the micro-wave oven. The sections were washed

in PBS (pH 7.4) for three times after the natural cooling. In order to block the

endogenous peroxidase, the sections were incubated with 3% hydrogen peroxide (H_2O_2) solutions for 20 min in the dark room and washed in PBS (pH 7.4) for three times. The washed sections were incubated with the primary antibody (1:1000 diluted with 5% bull serum albumin) overnight at 4°C and then incubated with corresponding horseradish peroxidase-conjugated (HRP) antibodies (CST, USA) for 50 min at the room temperature. After three times of washing, the sections were stained with diaminobenzidine (DAB) dye, counter stained with hematoxylin and examined by optical microscope (Olympus X71-F22PH, Japan). TF expression was identified as positively stained cytokines. Image pro-plus 6.0 software was used to calculate the integral optical density (IOD) to quantify the TF expression.

Cytokines measurement

Blood samples were collected with sodium citrate and were centrifuged at 2000 rpm for 5 min to obtain plasma. The expressions of von willebrand factor (vWF), P-selectin, TF, FXII, active coagulation factor X (FXa), thrombin-antithrombin complex (TAT), tissue factor pathway inhibitor (TFPI), antithrombin III (ATIII) and t-PA, D-dimer in the plasma of Wistar rats were measured by the corresponding enzyme-linked immunosorbent assay (ELISA) kits (Cusabio, USA) according to the instructions.

Western blot

100 mg of frozen lung tissue were ground completely with lysis buffer (Pierce, USA) and the protein extracts were quantified by performing the bicinchoninic acid (BCA) protein assay (Pierce, USA). Equal amounts of protein (80 μg) in different groups were loaded onto 12 % sodium dodecyl sulfate-polyacrylamide gel electrophoresis (SDS-PAGE) and

electrophoretically transferred to polyvinylidene fluoride (PVDF) membrane (Millipore,

USA). After blocking with 5 % nonfat milk in Tris-buffered saline (TBS) containing 0.05 %

Tween-20 (TBS-T) for 1 h at room temperature, the membrane incubated with

glyceraldehyde-phosphate dehydrogenase (GAPDH), TF, nuclear factor –κB/p65

(NF-κB/p65), phosphorylation- NF-κB (p-p65), c-Jun, phosphorylation -c-Jun (p-c-Jun),

c-Jun N-terminal kinase (JNK) rabbit antibodies (CST, USA) (1:1000 diluted) overnight at

4 °C, washed with TBS-T for three times, and incubated with horseradish

peroxidase-conjugated anti-Rabbit antibodies (CST, USA) (1:2000 diluted) for 1 h at room

temperature. After three times of washing with TBS-T, blots were processed using ECL kit

(Thermo Scientific, USA) and detected using Image LabTM Software (Bio-Rad Version 3.0,

USA).

Statistical analysis

Data were expressed as mean ± standard deviation (S.D.) and the significance of

statistical comparisons between experiment groups and control groups were determined by t

test using SPSS Statistics 21. The normal distribution of data was tested before performing t

test. Differences were considered significant at $*p < 0.05$.

Results

Characterization of silica nanoparticles

TEM was used to characterize the amorphous SiNPs and SiNPs appeared a spherical

shape and well dispersed (Figure 2A). The size distribution was measured by Image J

software and the average diameter of SiNPs was 52.05 ± 8.38 nm (Figure 2B). The average

hydrodynamic size of SiNPs in saline solution was 94.91 nm and the average value of Zeta

potential was -34.6 mv (Table 1). Our data suggested the good monodispersity of SiNPs in the

dispersion medium. The purity of SiNPs was confirmed higher than 99.9%.[18] The LAL assay

had not detected any endotoxin in all samples, showing negative results in SiNPs suspensions

(Table 2).

Coagulation parameters test

Figure 3 showed changes of coagulation parameters in SiNPs-treated and control

groups at 3 time points, APTT was significantly shortened at day 3 after consecutive

administration for a week, while PT didn't decline until day 7 ($p< 0.05$). At day 7, APPT in the

plasma of SiNPs-treated group recovered to normal level (Figure 3A and B). TT was

shortened at day 1, day 3 after intravenous injection of SiNPs ($p< 0.05$), and returned to

normal levels at day 7 (Figure 3C). The FIB contents in SiNPs-treated group were

significantly increased compared to those in control groups at any time point ($p< 0.05$), but a

gradual decrease of FIB content was found in the SiNPs-treated groups from day1 to day 7

(Figure 3D).

Detection of platelets activation

Figure 4A showed the amounts of platelets in whole blood of rats at 3 time points, the

number of platelets was significantly decreased at day 1 and day 3 ($p< 0.05$). As seen in

Figure 4B, platelet aggregation rates were significantly increased at 1, 3 and 7 days after

SiNPs treatment compared to the control groups respectively ($p< 0.05$). To evaluate the

structural changes of platelet membrane glucoproteins in rats, the expression levels of

FITC-CD42d (anti-GPV) and PE-CD61 (anti-GPIIIa) were detected. The positive expression

rates of CD42d tended to slightly decrease in a time manner from day 1 to day 7, sharing

lower levels than the control groups at all SiNPs-treated groups, however, the levels of CD61

showed the opposite trend with a significant increase compared to the control groups ($p< 0.05$)

(Figure 4C and D). Sustained increases in vWF and P-selectin release were discovered post

exposure at 3 time points (Figure 4E and F).

Measurement of coagulation factors

To further investigate how the extrinsic and intrinsic cascade pathways were initiated

and accelerated by SiNPs, the expression levels of coagulation factors in plasma of Wistar rats

were detected. As shown in Figure 5A, TF release was increased significantly at day1 after

treatment of SiNPs, slightly down-regulated at day 3, but still higher than the control group

($p< 0.05$), and at day 7, TF expression rose again, remarkably elevated compared to the

control group ($p< 0.05$). The content of FXII in the plasma increased significantly compared

to control group at day 1 after administration to SiNPs ($p< 0.05$), and from day 3 to day 7,

FXII levels fell down, no conspicuous differences were observed between the SiNPs-treated

and control groups (Figure 5B). As shown in Figure 5C, no significant difference in FXa

contents was found between the treatment and control group at day 1, but FXa expression

rose significantly at day 3 and day 7 ($p<0.05$). From our results, significant increases in TAT

levels were discovered at 3 time points after SiNPs exposure ($p< 0.05$), representing a

sustainably raised expression in thrombin generation (Figure 5D).

Histopathological examination

Lung sections of rats in control group showed normal lung mesh structure with normal

pulmonary epithelial cells, alveoli and alveoli septum, as well as pulmonary arterioles with

clean and smooth lumen (Figure 6A) (×200 magnification). Figure 6B (×200 magnification),

C and D (×400 magnification) showed lung tissue structure of rats at day 1 after SiNPs

treatment. Lung injury was discovered with destroyed alveoli, thickened alveoli septum and

many macrophages infiltrated in the alveolar septa and alveolar cavities. Large amounts of

fibrin exudation with SiNPs, deformed red cells and mononuclear inflammatory cells were

found in pulmonary arterioles.

TF Immunohistochemistry

To further trace the source of TF, immunohistochemical staining of TF in lung sections

was performed. In control groups, little positively stained cytokines were found in the fields

(Figure 7A) (×200 magnification). Figure 7B and C (×400 magnification) showed lots of

positively stained dots in the microvessels in lung sections, indicating strong expression of TF

induced by SiNPs in lung tissue. Figure 7D (×400 magnification) showed positive TF

expressions in small bronchi. In order to quantify the TF expression in lung tissue, we used

the IOD to measure the positive expression rates. As seen in Figure 7E, the SiNP-treated

groups showed significant increases in IOD value compared to the control group at three time

points, indicating that TF was strongly expressed in lung microcirculation.

Assessment of anti-coagulation and fibrinolytic resistance

To investigate whether anti-coagulation factors and fibrinolytic complements got

involved in maintaining the blood homeostasis, the expression levels of AT-III, TFPI, t-PA and

D-dimer were measured. As shown in Figure 8A, the plasma levels of AT-III in the

SiNPs-treated groups showed a declining trend in a time-dependent manner, significantly

decreased compared to those in control group at every time point ($p < 0.05$). From day 1 to

day 3, no observable differences of TFPI expression between treatment and control groups, but at day 7, levels of TFPI in SiNPs-treated group were obviously elevated ($p < 0.05$) (Figure 8B). Concentrations of t-PA and D-dimer in plasma after SiNPs treatment were higher than those in control groups at three time points ($p < 0.05$), especially the D-dimer levels increased significantly at day 7 (Figure 8C and D).

Molecular mechanism of pre-thrombotic state formation

To better understand the mechanism of SiNPs on pre-thrombotic state formation in rats, we examined the expression of TF activation related proteins by Western blot. As shown in Figure 9A, TF expression in SiNP-treated groups showed a significant increase at three time points ($p < 0.05$), which were highly consistent with the results of TF levels in plasma and immunohistochemical expression. From our data, SiNPs caused a significant increase in the phosphorylation expression of NF-κB/p65 at three time points compared to the control group ($p < 0.05$) (Figure 9B) and increased the phosphorylation expression of AP-1/c-Jun remarkably at the first day after injection ($p < 0.05$) (Figure 9C). As seen in Figure 9D, the protein expression level of JNK was increased significantly at day 1 after SiNPs administration ($p < 0.05$). Our data indicated that SiNPs could induce the TF expression by activating NF-κB and AP-1 transcription, and their upstream kinases (JNK) signaling pathway might involve in regulating the activation of NF-κB and AP-1.

Discussion

SiNPs have been widely utilized for medical application mainly through intravenous administration.[22,23] However, it could also cause adverse effects when SiNPs enter the

circulation by interacting with the blood components (blood cells, platelets, proteins and

coagulation factors) leading to coagulation disorders, worsening the prognosis of

cardiovascular diseases and accelerating its process to the formation of thrombotic

complications.[24] In this study, we focused on the time-course effects of intravenous exposure

to SiNPs on platelets function and blood coagulation in Wistar rats to investigate

pre-thrombotic effects of SiNPs *in vivo* and to detect the possible mechanism of

pre-thrombotic state.

Typical coagulation parameters in whole blood of rats were measured, including PT,

APTT, TT and FIB. PT measures the activity of extrinsic coagulation while APTT measures

the condition of intrinsic coagulation.[25] An epidemiological study on the effects of inhalable

PM on blood coagulation in Italy showed that PT was shortened, providing the evidence that

PM promoted the coagulation process and thrombin generation.[7] In this study, shortened

clotting time (Figure 3A and B) indicated that SiNPs resulted in hyperactivity of both the

extrinsic and intrinsic coagulation cascade, leading to a hypercoagulable state. FIB is one of

the most abundant coagulation factors, which can be transformed into fibrin under the

catalysis of thrombin, making a prominent contribution to the activation of coagulation

cascade. It was reported that $PM_{2.5}$ could enhance the FIB levels and increase the risk of acute

thrombosis.[26,27] Combined with the results of declined TT and elevated FIB levels (Figure 3C

and D), it was convinced that tiny blood clots were produced and SiNPs accelerated the

coagulation progress.

According to the Virchow's triad, cells (platelets and endothelial cells), blood proteins

(clotting/coagulation factors) and blood flow were considered as the three basic components,

working together to balance the pro-coagulant and anti-coagulant process.[28] Endothelial cells have been proven to get involved in various pathologic coagulation processes, such as atherosclerosis, deep venous thrombosis and myocardial infarction.[29] Previous studies found that amorphous SiNPs induced endothelial cells dysfunction through oxidative stress and inflammatory reaction via JNK/P53 and NF-κB pathways or induced autophagy via the PI3k/Akt/mTOR signaling pathway.[15,30] The cytokines of vWF are massively produced by injured endothelial cells and important for describing the endothelial function and highly related to platelets activation.[31] The increased levels of vWF in our study suggested that SiNPs could induce endothelial dysfunction *in vivo* (Figure 4E).

Platelets occupy an important position for maintaining blood stability, which can increase thrombin generation by leading to degranulation and changes of their amount, morphology and function.[19] It was reported that SiNPs (70nm) reduced the platelets amount in BALB/c mice, inducing consumptive coagulopathy.[32] The decreased platelets might owe to their consumption and destruction when SiNPs came into immediate contact with the platelets and activate them (Figure 4A). Blood is a complex fluid with abundant proteins, ions and blood cells. Nanoparticles can directly interact with blood proteins, resulting in the formation of a protein corona.[33] The surface properties alteration based on blood ionic strength can induce nanoparticle agglomerations, which retard cell motility and functions.[34] SiNPs agglomerations were possibly caused after translocation to the circulation, platelets could be activated via the increased opportunities of interacting between SiNPs with platelets surface and changing the function of proteins in platelets membrane. GPIIb/IIIa is recognized as an essential protein to mediate the aggregation of platelets via strong interaction with vWF,

giving enough capacity binding to fibrinogen.[35] GPIb-IX-V complex is crucial for platelet

adhesion and provides a natural ligand for thrombin, thereby the more thrombin produce, the

more GPIb-IX-V consume. Contrary to GPIIb/IIIa, GPIb-IX-V levels decrease with the

activation of platelets. Radomski et al found that exposure to carbon nanoparticles increased

human platelet aggregation via up-regulating GPIIb/IIIa activation and down-regulating the

GPIb expression *in vitro*.[12] Along with the high levels in the maximal platelet aggregator

response (Figure 4B), the structural of platelets membrane glucoproteins changed over time.

The decreased expression of CD42d (anti-GPV) and increased expression of CD61

(anti-GPIIIa) in this experiment indicated that SiNPs had the ability to aggregate platelets and

promote the adhesion of platelets *in vivo* (Figure 4C and D). P-selectin, which is a biomarker

of platelet activation, barely expresses in physiological conditions. However it has been

reported that MCN, MWCNT and SWCNT gave rise to a remarkable increase in P-selectin

release.[12] A sustained increase of P-selectin demonstrated SiNPs induced high activity of

platelets (Figure 4F). Our findings confirmed that SiNPs could trigger platelets activation via

aggregation and adhesion which is highly related to structural changes of platelets membrane

glucoproteins.

As well known, coagulation system can be directly activated either by an intrinsic

pathway initiated through FXII activation, or by an extrinsic pathway triggered by TF. It has

been reported that SiNPs (20 nm) induced coagulopathy that PT were shortened but no

changes of APTT were found during the experiment.[25] Nanoparticles of larger size could

provide more active surface and directly contact with FXII to initiate the intrinsic pathway,

and moreover the anionic nanoparticles with negative superficial charge have more potential

17

to bind with FXII.[36] Pro-coagulant activities were decreased in the FXII-deficient plasma[32] and we have discovered that SiNPs induced the activation of FXII in the plasma of rats (Figure 5B), these results suggested that FXII was an essential factor to accelerate the blood coagulation and the interaction between SiNPs with FXII was crucial to the biological effects. TF is a cell-surface glycoprotein, mainly released from monocytes, macrophages and damaged endothelial cells in circulating blood.[37] Exposed TF forms a complex by binding with the natural ligand FVII, namely TF-FVIIa complex, which further converts the FX to its activated forms and contributes to variety of pre-thrombotic syndromes, such as atherosclerosis, angiogenesis and DIC.[38-41] TF expression was increased after intravenous administration to SiNPs but not after intranasal exposure,[13,32] this might due to the fact that low blood levels of SiNPs through intranasal administration cannot induce a drastic release of TF. In our experiment, SiNPs induced a sustained and potent increase in TF expression in plasma and lung sections (Figure 5A and Figure 7). The lung tissue was chosen mainly due to the abundance of microvessels and monocyte-macrophages, where the TF originally expressed. The strong expression of TF in immunohistochemistry slides indicated that SiNPs could induce endothelial dysfunction and monocyte-macrophages proliferation, leading to coagulation disorder.

FXa is the initiator of common coagulation pathway, involving in forming the prothrombin complex. FXa can be activated by TF-FVIIa complex and by contacting with intrinsic coagulation factors. Our data showed that FXa ascended sharply from the third day, since then common coagulation pathway was fully activated (Figure 5C). Usually, the thrombin remains stable by TAT formation, so the TAT levels in plasma are generally

regarded as a sensible marker for evaluation of the early thrombin production.[42] In this study,

significant increases in TAT levels were discovered (Figure 5D), thus thrombin was produced

remarkably. FIB can be converted to fibrin under the catalysis of thrombin, it make sense that

FIB in SiNPs-treated groups appeared a declined trend (Figure 4D). Our study on the

coagulation system suggested that SiNPs induced a large release and comprehensive

activation of coagulation factors, leading to hypercoagulable state.

There are abundant microcirculations in lung tissue of rats, histopathological

examination in lung sections showed plenty of pink fibrin exudation, deformed red cells and

monocytes (Figure 6B and D). The exudation was too loose and transparent to be treated as

thrombus, given the changes of platelets function and coagulation system, pre-thrombotic

state was considered to be caused by SiNPs. The pre-thrombotic state are consequences of

increased blood viscosity, platelets activation, coagulation hyperfunction, anti-coagulation

and fibrinolytic resistance. As same as envisioned, anti-coagulation and fibrinolytic resistance

contributed to the pre-thrombotic effect of SiNPs as well in our experiment. AT-III, as the

most important natural anticoagulant in mammalian systems, plays a critical role in

controlling the activity of thrombin and inhibiting the viability of coagulation factors.[43] AT-III

was found at a significantly low level in septic patients with DIC, consequently accelerated

the coagulation cascade activation and thrombosis generation.[44] The gradually downward

trend in AT-III content (Figure 8A) showed a low anticoagulant ability leading to the

hypercoagulable state caused by SiNPs. TFPI is a specific inhibitor of TF, low levels of TFPI

could raise the risk of the first and recurrent VET (Venous Thrombus Embolism) and

stroke.[45,46] In our study, TFPI expression didn't show a significant change in the beginning,

indicating that SiNPs induced low anti-coagulant ability failing to fight for the high levels of

TF, then TFPI increased at day 7 (Figure 8B), we proposed that a physiological anticoagulant

response happened to resist the extrinsic coagulation cascade activation.

The t-PA is a key enzyme in fibrinolysis due to its remarkable ability to mediate the

plasminogen cleavage and plasmin regeneration, ultimately induce the fibrin degradation.[47]

Usually the immunoassay of t-PA antigen measures the circulating complex between t-PA and

its particular inhibitor (plasminogen activator inhibitor-1, PAI-1), the inhibition of PAI-1

increased with the high levels of t-PA, t-PA actually showed low activity.[7] The elevation of

t-PA levels in our experiment was explained to reduce the fibrinolytic activity to strengthen

blood coagulation (Figure 8C). D-dimer is the minimum protein fragment degraded from

cross-linked fibrin via fibrinolysis, usually considered as a sensitive marker of indicating

hypercoagulable state and secondary hyperfibrinolysis of DIC.[48,49] It has been found that a

significant increase in D-dimer levels in plasma of Wistar rats after intratracheal instillation of

four kinds of silica particles (30, 60, 90 and 600 nm), and the D-dimer levels in the SiNPs

groups were much higher than that in Si600 group.[14] In this experiment, the elevated release

of D-dimer demonstrated SiNPs induced hypercoagulation and secondary hyperfibrinolysis in

rats (Figure 8D). From the present findings, it can be inferred that anti-coagulation and

fibrinolytic resistance were involved in regulation the pre-thrombotic state formation through

the consumption of anti-coagulant factors and low activity of fibrinolysis. Anti-coagulation

and fibrinolytic resistance can be a new research target for prevention from coagulation

disorder caused by SiNPs as drug delivery.

Based on the results of TF expression and FXII levels, we believed SiNPs can induce

hypercoagulable state both by initiating intrinsic and extrinsic pathway. As mentioned above,

the interaction between SiNPs with FXII is crucial to the pre-thrombotic effects induced by

SiNPs, further promoting the initiation of coagulation cascade and the activation of

coagulation factors. SiNPs induced obvious increases in TF expression in our study, the

signaling pathway governing TF activation were considered as the reasonable explanation for

pre-thrombotic state formation. It was reported that NF-κB and AP-1 were essential

transcription sites for inducible activation of *F3* gene to synthesize TF.[50,51] NF-κB family,

including RelA (p65), c-Rel, RelB, NF-κB1 (p50), and NF-κB2 (p52), originally emerged as a

major regulator of immune response to infection[52] while AP-1 generally consists of JUN and

FOS protein families as its main basic leucine domain.[53] NF-κB/p65 and AP-1/c-Jun were

confirmed necessary for full-scope TF (*F3*) activation at the transcriptional level in human

tissue.[51] Our data of increased phosphorylation of NF-κB/p65 and AP-1/c-Jun indicated that

SiNPs up-regulated TF expression via the activation of NF-κB and AP-1 signaling (Figure 9B

and C). NF-κB and AP-1 can be up-regulated in response of the activation of several upstream

pathways, Erk1/2, JNK, and p38 MAPK pathways were extensively involved.[54] Our group

has found that JNK pathway was remarkably phosphorylated to activate NF-κB signaling to

reply oxidative stress oxidative stress and inflammatory reaction caused by SiNPs in

endothelia cells.[55] In this experiment, JNK pathway was activated as a possible

upstream-regulated mechanism of NF-κB and AP-1 transcription (Figure 9D), and JNK-

NF-κB/ AP-1 pathway was regarded as the possible mechanism of pre-thrombotic state

induced by SiNPs.

Conclusions

In summary, our results showed that intravenous administration of SiNPs caused the hypercoagulable and pre-thrombotic state in rats. The pre-thrombotic induced by SiNPs state via the interaction between endothelial cells damages, platelets activation, coagulation system hyperfunction, the consumption of anti-coagulation factors and fibrinolytic resistance. Direction interaction between SiNPs and FXII as well as the activation of JNK-NF-κB/AP-1 pathway were responsible for pre-thrombotic state formation. The pre-thrombotic state we discussed gave a new insight into the knowledge of the hemostability and biocompatibility of SiNPs and more studies on adverse effects and the biomedical mechanism of SiNPs in medical application are still needed

Author Contributions

Conceived and designed the experiments: Lizhen Jiang and Zhiwei Sun. Performed the experiments: Lizhen Jiang, Yanbo Li, Caixia Guo, Yongbo Yu, Yang Zou, Yang Yu, Junchao

Duan, Weijia Geng, Qiuling Li. Analyzed the data: Lizhen Jiang, Yang Li and Yumei Yang.

Wrote the manuscript: Lizhen Jiang

Disclosure

The authors declare they have no actual or potential competing financial interests.

References

1. Park EJ, Park K. Oxidative stress and pro-inflammatory responses induced by silica nanoparticles in vivo and in vitro. *Toxicol Lett*. 2009;184(1):18-25.
2. Rosenholm JM, Sahlgren C, Linden M. Towards multifunctional, targeted drug delivery systems using mesoporous silica nanoparticles--opportunities & challenges. *Nanoscale*. 2010;2(10):1870-1883.
3. Cho M, Cho WS, Choi M, Kim SJ, Han BS, Kim SH, Kim HO, Sheen YY, Jeong J. The impact of size on tissue distribution and elimination by single intravenous injection of silica nanoparticles. *Toxicol Lett*. 2009;189(3):177-183.
4. LeBlanc AJ, Cumpston JL, Chen BT, Frazer D, Castranova V, Nurkiewicz TR. Nanoparticle inhalation impairs endothelium-dependent vasodilation in subepicardial arterioles. *J Toxicol Environ Health A*. 2009;72(24):1576-1584.
5. Crosera M, Bovenzi M, Maina G, Adami G, Zanette C, Florio C, Filon Larese F. Nanoparticle dermal absorption and toxicity: a review of the literature. *Int Arch Occup Environ Health*. 2009;82(9):1043-1055.
6. Brook RD, Rajagopalan S, Pope CA, 3rd, Brook JR, Bhatnagar A, Diez-Roux AV, Holguin F, Hong Y, Luepker RV, Mittleman MA, Peters A, Siscovick D, Smith SC, Jr., Whitsel L, Kaufman JD, American Heart Association Council on E, Prevention CotKiCD, Council on Nutrition PA, Metabolism. Particulate matter air pollution and cardiovascular disease: An update to the scientific statement from the American Heart Association. *Circulation*. 2010;121(21):2331-2378.
7. Bonzini M, Tripodi A, Artoni A, Tarantini L, Marinelli B, Bertazzi PA, Apostoli P, Baccarelli A. Effects of inhalable particulate matter on blood coagulation. *J Thromb Haemost*. 2010;8(4):662-668.
8. Geys J, Nemmar A, Verbeken E, Smolders E, Ratoi M, Hoylaerts MF, Nemery B, Hoet PH. Acute toxicity and prothrombotic effects of quantum dots: impact of surface charge. *Environ Health Perspect*. 2008;116(12):1607-1613.
9. Jun EA, Lim KM, Kim K, Bae ON, Noh JY, Chung KH, Chung JH. Silver nanoparticles enhance thrombus formation through increased platelet aggregation and procoagulant activity. *Nanotoxicology*. 2011;5(2):157-167.
10. Yamashita K, Yoshioka Y, Higashisaka K, Mimura K, Morishita Y, Nozaki M, Yoshida T, Ogura T, Nabeshi H, Nagano K, Abe Y, Kamada H, Monobe Y, Imazawa T, Aoshima H, Shishido K, Kawai Y, Mayumi T, Tsunoda S, Itoh N, Yoshikawa T, Yanagihara I, Saito S, Tsutsumi Y. Silica and titanium dioxide nanoparticles cause pregnancy complications in mice. *Nat Nanotechnol*. 2011;6(5):321-328.

11. Bihari P, Holzer M, Praetner M, Fent J, Lerchenberger M, Reichel CA, Rehberg M, Lakatos S, Krombach F. Single-walled carbon nanotubes activate platelets and accelerate thrombus formation in the microcirculation. *Toxicology*. 2010;269(2-3):148-154.

12. Radomski A, Jurasz P, Alonso-Escolano D, Drews M, Morandi M, Malinski T, Radomski MW. Nanoparticle-induced platelet aggregation and vascular thrombosis. *Br J Pharmacol*. 2005;146(6):882-893.

13. Yoshida T, Yoshioka Y, Tochigi S, Hirai T, Uji M, Ichihashi K, Nagano K, Abe Y, Kamada H, Tsunoda S, Nabeshi H, Higashisaka K, Yoshikawa T, Tsutsumi Y. Intranasal exposure to amorphous nanosilica particles could activate intrinsic coagulation cascade and platelets in mice. *Part Fibre Toxicol*. 2013;10:41.

14. Du Z, Zhao D, Jing L, Cui G, Jin M, Li Y, Liu X, Liu Y, Du H, Guo C, Zhou X, Sun Z. Cardiovascular toxicity of different sizes amorphous silica nanoparticles in rats after intratracheal instillation. *Cardiovasc Toxicol*. 2013;13(3):194-207.

15. Liu X, Sun J. Endothelial cells dysfunction induced by silica nanoparticles through oxidative stress via JNK/P53 and NF-kappaB pathways. *Biomaterials*. 2010;31(32):8198-8209.

16. Gwinn MR, Vallyathan V. Nanoparticles: health effects--pros and cons. *Environ Health Perspect*. 2006;114(12):1818-1825.

17. Duan J, Yu Y, Li Y, Yu Y, Sun Z. Cardiovascular toxicity evaluation of silica nanoparticles in endothelial cells and zebrafish model. *Biomaterials*. 2013;34(23):5853-5862.

18. Yu Y, Li Y, Wang W, Jin M, Du Z, Li Y, Duan J, Yu Y, Sun Z. Acute toxicity of amorphous silica nanoparticles in intravenously exposed ICR mice. *PLoS One*. 2013;8(4):e61346.

19. Ilinskaya AN, Dobrovolskaia MA. Nanoparticles and the blood coagulation system. Part I: benefits of nanotechnology. *Nanomedicine (Lond)*. 2013;8(5):773-784.

20. Ilinskaya AN, Dobrovolskaia MA. Nanoparticles and the blood coagulation system. Part II: safety concerns. *Nanomedicine (Lond)*. 2013;8(6):969-981.

21. Sun L, Li Y, Liu X, Jin M, Zhang L, Du Z, Guo C, Huang P, Sun Z. Cytotoxicity and mitochondrial damage caused by silica nanoparticles. *Toxicol In Vitro*. 2011;25(8):1619-1629.

22. Duncan R, Gaspar R. Nanomedicine(s) under the microscope. *Mol Pharm*. 2011;8(6):2101-2141.

23. Slowing, II, Vivero-Escoto JL, Wu CW, Lin VS. Mesoporous silica nanoparticles as controlled release drug delivery and gene transfection carriers. *Adv Drug Deliv Rev*. 2008;60(11):1278-1288.

24. Utell MJ, Frampton MW, Zareba W, Devlin RB, Cascio WE. Cardiovascular effects associated with air pollution: potential mechanisms and methods of testing. *Inhal Toxicol*. 2002;14(12):1231-1247.

25. Liu X, Sun J. Time-course effects of intravenously administered silica nanoparticles on blood coagulation and endothelial function in rats. *J Nanosci Nanotechnol*. 2013;13(1):222-228.

26. Peters A, Frohlich M, Doring A, Immervoll T, Wichmann HE, Hutchinson WL, Pepys MB, Koenig W. Particulate air pollution is associated with an acute phase response in men; results from the MONICA-Augsburg Study. *Eur Heart J*. 2001;22(14):1198-1204.

27. Medeiros N, Jr., Rivero DH, Kasahara DI, Saiki M, Godleski JJ, Koutrakis P, Capelozzi VL, Saldiva PH, Antonangelo L. Acute pulmonary and hematological effects of two types of particle surrogates are influenced by their elemental composition. *Environ Res*. 2004;95(1):62-70.

28. Wang L, Li J, Jiang Q, Zhao L. Water-soluble Fe3O4 nanoparticles with high solubility for removal of heavy-metal ions from waste water. *Dalton Trans*. 2012;41(15):4544-4551.

29. Davda J, Labhasetwar V. Characterization of nanoparticle uptake by endothelial cells. *Int J Pharm*. 2002;233(1-2):51-59.

30. Duan J, Yu Y, Yu Y, Li Y, Wang J, Geng W, Jiang L, Li Q, Zhou X, Sun Z. Silica nanoparticles induce autophagy and endothelial dysfunction via the PI3K/Akt/mTOR signaling pathway. *Int J Nanomedicine*. 2014;9:5131-5141.

31. Montoro-Garcia S, Shantsila E, Lip GY. Potential value of targeting von Willebrand factor in atherosclerotic cardiovascular disease. *Expert Opin Ther Targets*. 2014;18(1):43-53.

32. Nabeshi H, Yoshikawa T, Matsuyama K, Nakazato Y, Arimori A, Isobe M, Tochigi S, Kondoh S, Hirai T, Akase T, Yamashita T, Yamashita K, Yoshida T, Nagano K, Abe Y, Yoshioka Y, Kamada H, Imazawa T, Itoh N, Kondoh M, Yagi K, Mayumi T, Tsunoda S, Tsutsumi Y. Amorphous nanosilicas induce consumptive coagulopathy after systemic exposure. *Nanotechnology*. 2012;23(4):045101.

33. Casals E, Pfaller T, Duschl A, Oostingh GJ, Puntes V. Time evolution of the nanoparticle protein corona. *ACS Nano*. 2010;4(7):3623-3632.

34. Lacerda SH, Park JJ, Meuse C, Pristinski D, Becker ML, Karim A, Douglas JF. Interaction of gold nanoparticles with common human blood proteins. *ACS Nano*. 2010;4(1):365-379.

35. Madan M, Berkowitz SD, Christie DJ, Smit AC, Sigmon KN, Tcheng JE. Determination of platelet aggregation inhibition during percutaneous coronary intervention with the platelet function analyzer PFA-100. *Am Heart J*. 2002;144(1):151-158.

36. Oslakovic C, Cedervall T, Linse S, Dahlback B. Polystyrene nanoparticles affecting blood coagulation. *Nanomedicine*. 2012;8(6):981-986.

37. Scholefield H. Best Practice and Research Clinical Obstetrics and Gynaecology. Preface. *Best Pract Res Clin Obstet Gynaecol*. 2008;22(5):761-762.

38. Bogdanov VY, Balasubramanian V, Hathcock J, Vele O, Lieb M, Nemerson Y. Alternatively spliced human tissue factor: a circulating, soluble, thrombogenic protein. *Nat Med*. 2003;9(4):458-462.

39. van den Berg YW, Osanto S, Reitsma PH, Versteeg HH. The relationship between tissue factor and cancer progression: insights from bench and bedside. *Blood*. 2012;119(4):924-932.

40. Rattray DD, O'Connell CM, Baskett TF. Acute disseminated intravascular coagulation in obstetrics: a tertiary centre population review (1980 to 2009). *J Obstet Gynaecol Can*. 2012;34(4):341-347.

41. Steffel J, Luscher TF, Tanner FC. Tissue factor in cardiovascular diseases: molecular mechanisms and clinical implications. *Circulation*. 2006;113(5):722-731.

42. Giordano P, Del Vecchio GC, Cecinati V, Delvecchio M, Altomare M, De Palma F, De Mattia D, Cavallo L, Faienza MF. Metabolic, inflammatory, endothelial and haemostatic markers in a group of Italian obese children and adolescents. *Eur J Pediatr*. 2011;170(7):845-850.

43. Quinsey NS, Greedy AL, Bottomley SP, Whisstock JC, Pike RN. Antithrombin: in control of coagulation. *Int J Biochem Cell Biol*. 2004;36(3):386-389.

44. Iba T, Saito D, Wada H, Asakura H. Efficacy and bleeding risk of antithrombin supplementation in septic disseminated intravascular coagulation: a prospective multicenter survey. *Thromb Res*. 2012;130(3):e129-133.

45. Lwaleed BA, Bass PS. Tissue factor pathway inhibitor: structure, biology and involvement in disease. *J Pathol*. 2006;208(3):327-339.

46. Maroney SA, Mast AE. Expression of tissue factor pathway inhibitor by endothelial cells and platelets. *Transfus Apher Sci*. 2008;38(1):9-14.

47. Carmeliet P, Schoonjans L, Kieckens L, Ream B, Degen J, Bronson R, De Vos R, van den Oord JJ, Collen D, Mulligan RC. Physiological consequences of loss of plasminogen activator gene function in mice. *Nature*. 1994;368(6470):419-424.

48. Vene N, Mavri A, Kosmelj K, Stegnar M. High D-dimer levels predict cardiovascular events in patients with chronic atrial fibrillation during oral anticoagulant therapy. *Thromb Haemost*. 2003;90(6):1163-1172.

49. Wells PS, Anderson DR, Rodger M, Forgie M, Kearon C, Dreyer J, Kovacs G, Mitchell M, Lewandowski B, Kovacs MJ. Evaluation of D-dimer in the diagnosis of suspected deep-vein thrombosis. *N Engl J Med*. 2003;349(13):1227-1235.

50. Koo JW, Russo SJ, Ferguson D, Nestler EJ, Duman RS. Nuclear factor-kappaB is a critical mediator of stress-impaired neurogenesis and depressive behavior. *Proc Natl Acad Sci U S A*. 2010;107(6):2669-2674.

51. Sovershaev TA, Egorina EM, Unruh D, Bogdanov VY, Hansen JB, Sovershaev MA. BMP-7 induces TF expression in human monocytes by increasing F3 transcriptional activity. *Thromb Res*. 2015;135(2):398-403.

52. Wang S, Liu Z, Wang L, Zhang X. NF-kappaB signaling pathway, inflammation and colorectal cancer. *Cell Mol Immunol*. 2009;6(5):327-334.

53. Jiang J, Slivova V, Jedinak A, Sliva D. Gossypol inhibits growth, invasiveness, and angiogenesis in human prostate cancer cells by modulating NF-kappaB/AP-1 dependent- and independent-signaling. *Clin Exp Metastasis*. 2012;29(2):165-178.

54. Vaiopoulos AG, Papachroni KK, Papavassiliou AG. Colon carcinogenesis: Learning from NF-kappaB and AP-1. *Int J Biochem Cell Biol*. 2010;42(7):1061-1065.

55. Guo C, Xia Y, Niu P, Jiang L, Duan J, Yu Y, Zhou X, Li Y, Sun Z. Silica nanoparticles induce oxidative stress, inflammation, and endothelial dysfunction in vitro via activation of the MAPK/Nrf2 pathway and nuclear factor-kappaB signaling. *Int J Nanomedicine*. 2015;10:1463-1477.

Table 1 Hydrodynamic size and Zeta potential of SiNPs in physiological saline with different
concentrations

Concentration	Size (nm)	Zeta potential (mv)	PDI
500 μg/mL	94.18±1.65	-37.3±3.18	0.112
250 μg/mL	95.31±4.20	-32.5±3.03	0.103
125 μg/mL	95.13±2.47	-34.0±2.95	0.095

Table 2 Results of endotoxin detection by LAL assay

Concentration (mg/mL)	Sample	Sample + Positive Control	Positive Control	Negative Control
0.75	−	+	+	−
1.5	−	+	+	−
3	−	+	+	−
6	−	+	+	−
12	−	+	+	−

(−): negative   (+): positive

Figure 1. Experimental design of hematotoxicity of silica nanoparticles in Wistar rats.

Figure 2. Characterization of the silica nanoparticles (SiNPs). (A) Transmission electron microscope (TEM) image of SiNPs in physiological saline as the dispersion media: the particles appeared spherical and well dispersed. (Scale bar: 50 nm). (B) The size distribution of SiNPs calculated by Image J software.

Figure 3. The coagulation parameters test at 3 time points after intravenous injection of silica nanoparticles (SiNPs) for 7 days. (A) Prothrombin time (PT); (B) Activated partial thromboplastin time (APTT); (C) Thrombin time (TT); (D) Fibrinogen (FIB). Data represent mean ± S.D.,*$p < 0.05$ vs control group.

Figure 4. The effects of silica nanoparticles (SiNPs) on platelets function in blood plasma of rats at 3 time points after intravenous injection for 7 days. (A) Platelets number was detected by Veterinary Blood Analyzer. (B) Platelets aggregation rates measured by LBY-NJ4 Semi-automatic Platelet Aggregometer. (C) The positive expression rates of CD42d (%) and (D) the positive expression rates of CD61 (%) detected by flow cytometry. (E) Von willebrand factor (vWF) and (F) P-selectin expression measured by ELISA. Data are expressed as mean ± S.D., *$p < 0.05$ vs control group.

Figure 5. The effects of silica nanoparticles (SiNPs) on coagulation system in Wistar rats at 3 time points after intravenous injection for 7 days. (A) Tissue factor (TF) expression; (B) Coagulation factor XII (F XII) expression; (C) Active coagulation factor X (F Xa) expression; (D) Thrombin-antithrombin complex (TAT) expression. Data are expressed as mean ± S.D., *$p < 0.05$ vs control group.

Figure 6. Histological examination of lung tissue. Representative pictures from hematoxylin and eosin (HE) staining sections at day 1 after intravenous injection of silica nanoparticles (SiNPs). (A) Control group; (B),(C),(D) SiNPs-treated group. Black arrows denote abnormal pulmonary vessels within deformed red cells, inflammatory cells and fibrin exudation. The magnification was ×200 for (A) and (B), ×400 for (C) and (D).

Figure 7. Immunohistochemistry stain of tissue factor (TF). Representative pictures from immunohistochemically stained lung sections after intravenous injection of silica nanoparticles (SiNPs). (A) Control group; (B),(C),(D) SiNPs-treated group. Black arrows denote positively stained cytokines in pulmonary vessels and Bronchi. The magnification was ×200 for (A) and (D), ×400 for (B) and (C). (E) Quantitative determination of positive expression in immunohistochemical slides. Data are expressed as mean ± S.D., *$p < 0.05$ vs control group.

Figure 8. The effects of silica nanoparticles (SiNPs) on anti-coagulation and fibrinolytic system in Wistar rat s at 3 time points after intravenous injection for 7 days. (A) Antithrombin III (AT-III) expression; (B) Tissue factor pathway inhibitor (TFPI) expression; (C) Tissue plasminogen activator (t-PA) expression; (D) D-dimer expression. Data are expressed as mean ± S.D., *$p < 0.05$ vs control group.

Figure 9. The molecular mechanism involving in regulating tissue factor (TF) expression in lung tissue after intravenous injection of silica nanoparticles (SiNPs). (A) TF expression; (B) The phosphorylation expression of nuclear factor-κB/p65 (NF-κB/p65); (C) Phosphorylation expression of activator protein-1/ c-Jun (AP-1/c-Jun); (D) The protein levels of c-Jun N-terminal kinase (JNK) measured by Western blot. Data are expressed as mean ± S.D., *$p < 0.05$ vs control group.
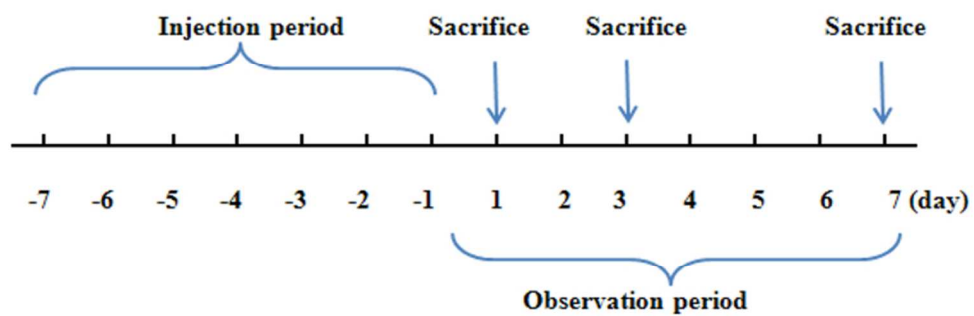
Figure 1. Experimental design of hematotoxicity of silica nanoparticles in Wistar rats.
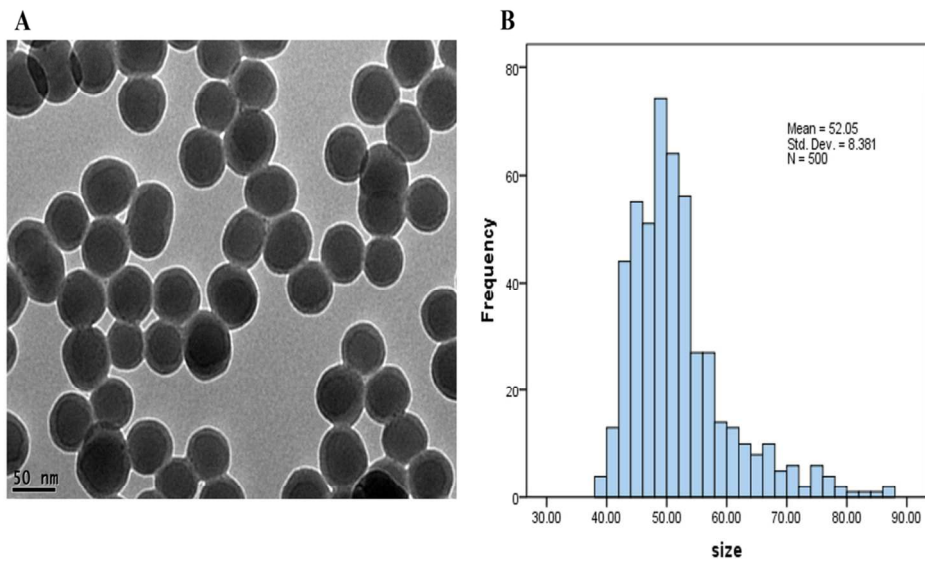68x27mm (300 x 300 DPI)

Figure 2. Characterization of the silica nanoparticles (SiNPs). (A) Transmission electron microscope (TEM) image of SiNPs in physiological saline as the dispersion media: the particles appeared spherical and well dispersed. (Scale bar: 50 nm). (B) The size distribution of SiNPs calculated by Image J software.
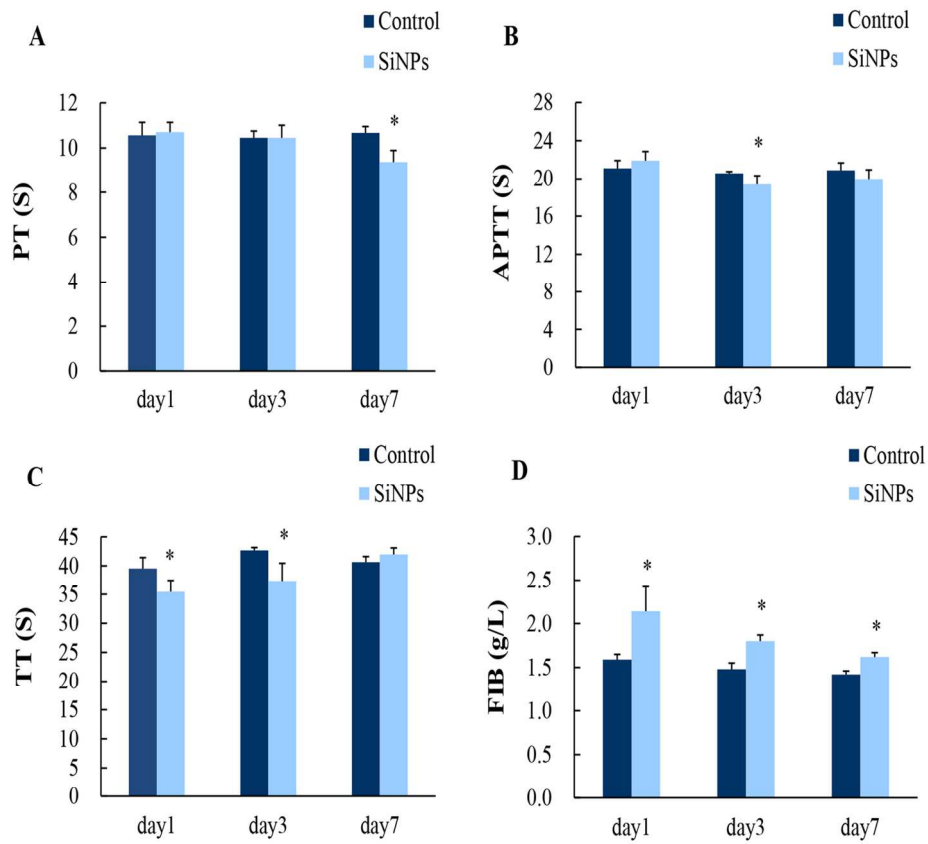99x58mm (300 x 300 DPI)

Figure 3. The coagulation parameters test at 3 time points after intravenous injection of silica nanoparticles (SiNPs) for 7 days. (A) Prothrombin time (PT); (B) Activated partial thromboplastin time (APTT); (C) Thrombin time (TT); (D) Fibrinogen (FIB). Data represent mean ± S.D.,*p< 0.05 vs control group.
153x139mm (300 x 300 DPI)

Figure 4. The effects of silica nanoparticles (SiNPs) on platelets function in blood plasma of rats at 3 time points after intravenous injection for 7 days. (A) Platelets number was detected by Veterinary Blood Analyzer. (B) Platelets aggregation rates measured by LBY-NJ4 Semi-automatic Platelet Aggregometer. (C) The positive expression rates of CD42d (%) and (D) the positive expression rates of CD61 (%) detected by flow cytometry. (E) Von willebrand factor (vWF) and (F) P-selectin expression measured by ELISA. Data are expressed as mean ± S.D., *p< 0.05 vs control group.
219x284mm (300 x 300 DPI)
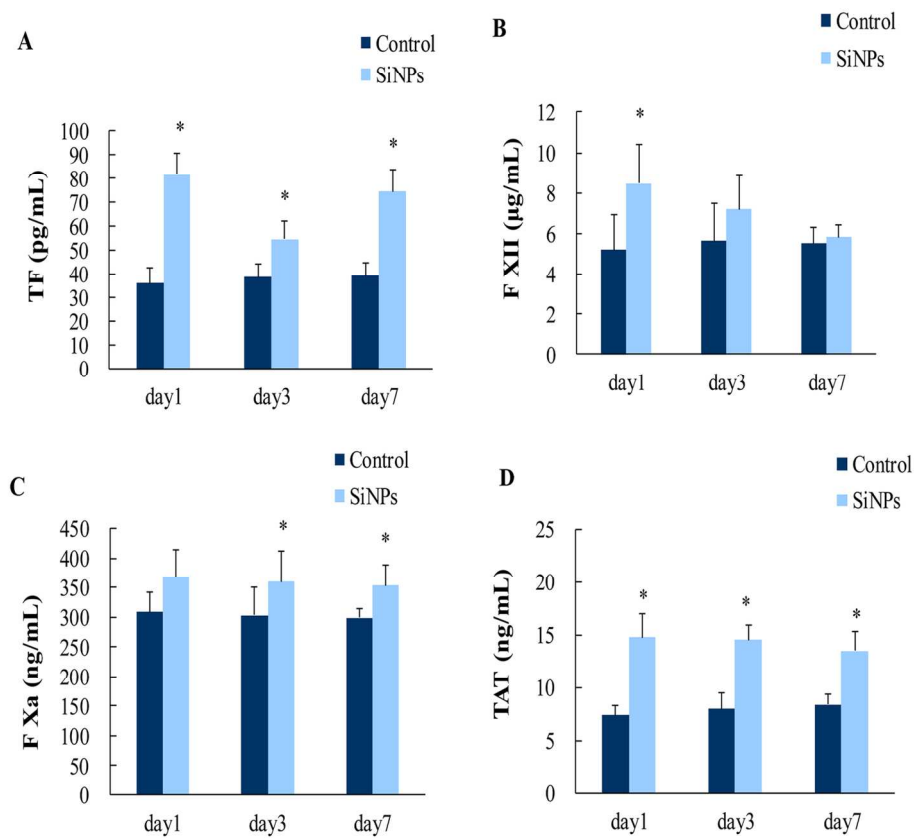
Figure 5. The effects of silica nanoparticles (SiNPs) on coagulation system in Wistar rats at 3 time points after intravenous injection for 7 days. (A) Tissue factor (TF) expression; (B) Coagulation factor XII (F XII) expression; (C) Active coagulation factor X (F Xa) expression; (D) Thrombin-antithrombin complex (TAT) expression. Data are expressed as mean ± S.D., *p< 0.05 vs control group.
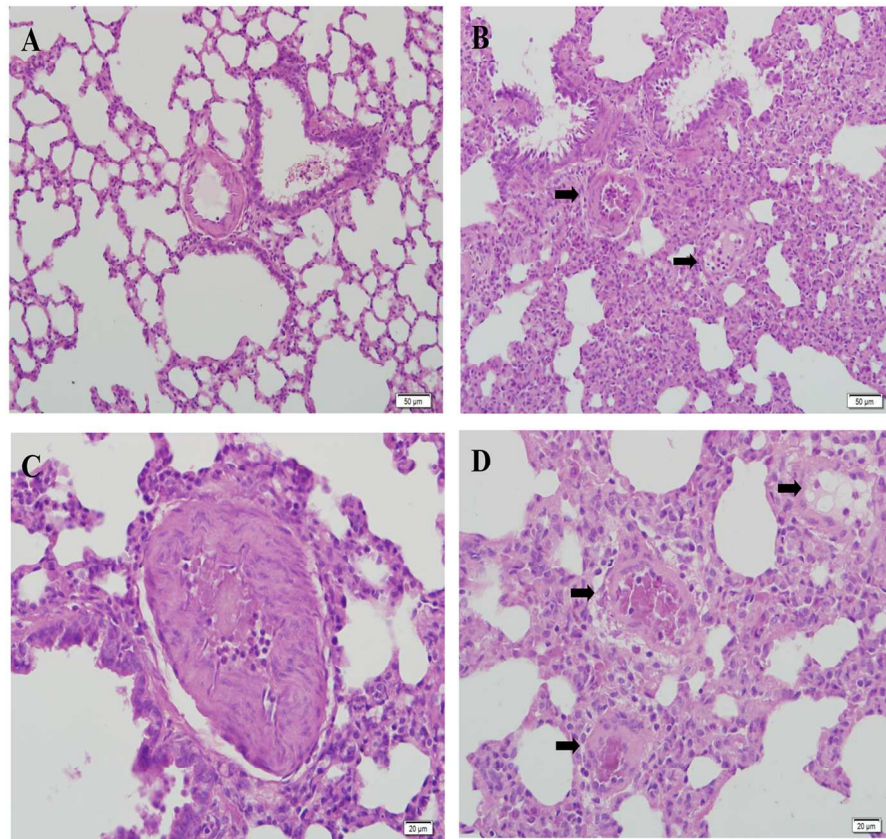153x139mm (300 x 300 DPI)

Figure 6. Histological examination of lung tissue. Representative pictures from hematoxylin and eosin (HE) staining sections at day 1 after intravenous injection of silica nanoparticles (SiNPs). (A) Control group; (B),(C),(D) SiNPs-treated group. Black arrows denote abnormal pulmonary vessels within deformed red cells, inflammatory cells and fibrin exudation. The magnification was ×200 for (A) and (B), ×400 for (C) and (D).
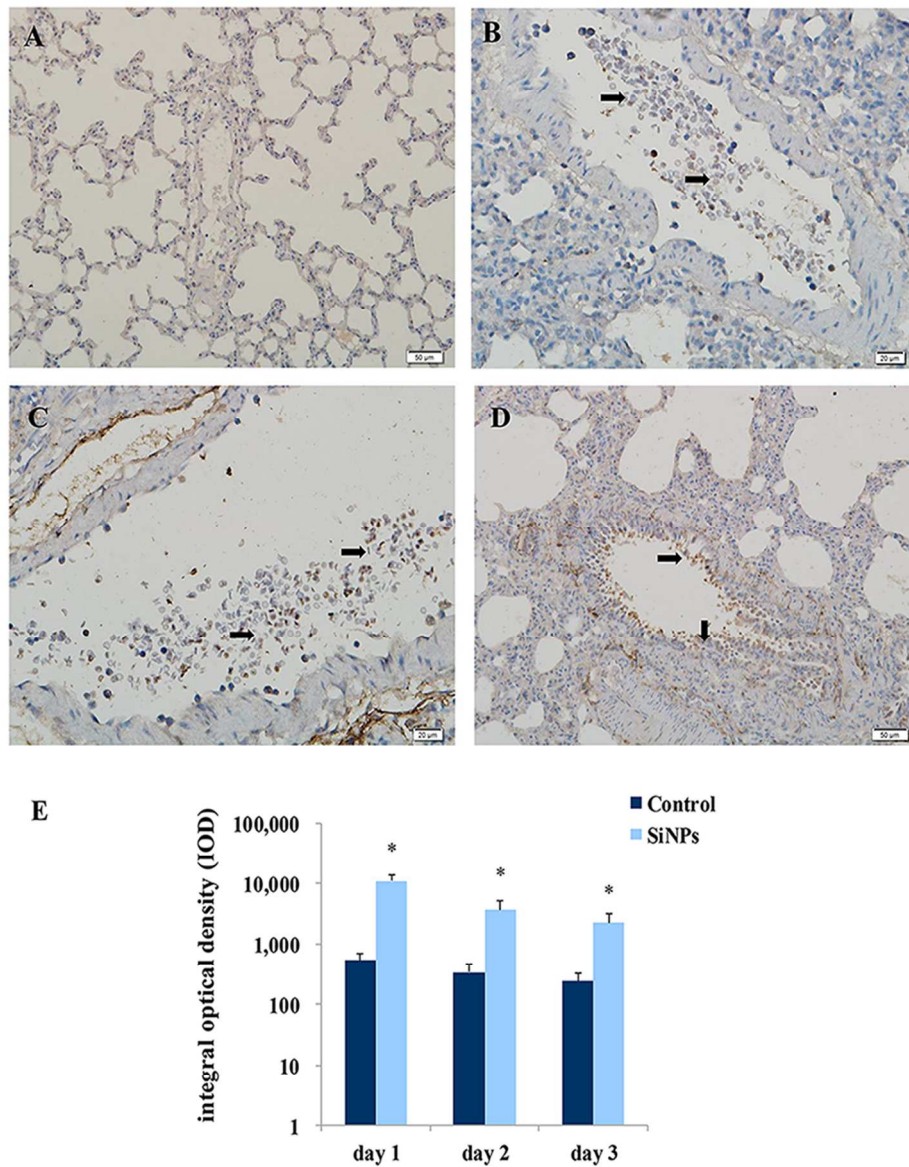153x139mm (300 x 300 DPI)

Figure 7. Immunohistochemistry stain of tissue factor (TF). Representative pictures from immunohistochemically stained lung sections after intravenous injection of silica nanoparticles (SiNPs). (A) Control group; (B),(C),(D) SiNPs-treated group. Black arrows denote positively stained cytokines in pulmonary vessels and Bronchi. The magnification was ×200 for (A) and (D), ×400 for (B) and (C). (E) Quantitative determination of positive expression in immunohistochemical slides. Data are expressed as mean ± S.D., *p< 0.05 vs control group.
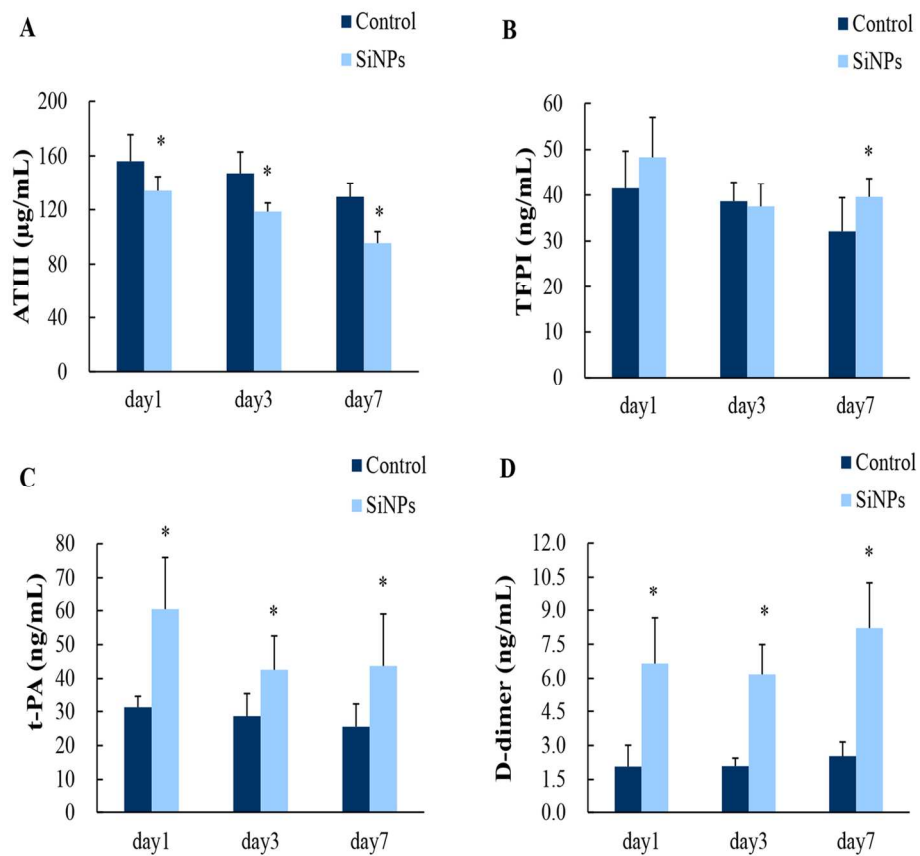170x209mm (300 x 300 DPI)

Figure 8. The effects of silica nanoparticles (SiNPs) on anti-coagulation and fibrinolytic system in Wistar rat s at 3 time points after intravenous injection for 7 days. (A) Antithrombin III (AT-III) expression; (B) Tissue factor pathway inhibitor (TFPI) expression; (C) Tissue plasminogen activator (t-PA) expression; (D) D-dimer expression. Data are expressed as mean ± S.D., *$p < 0.05$ vs control group.
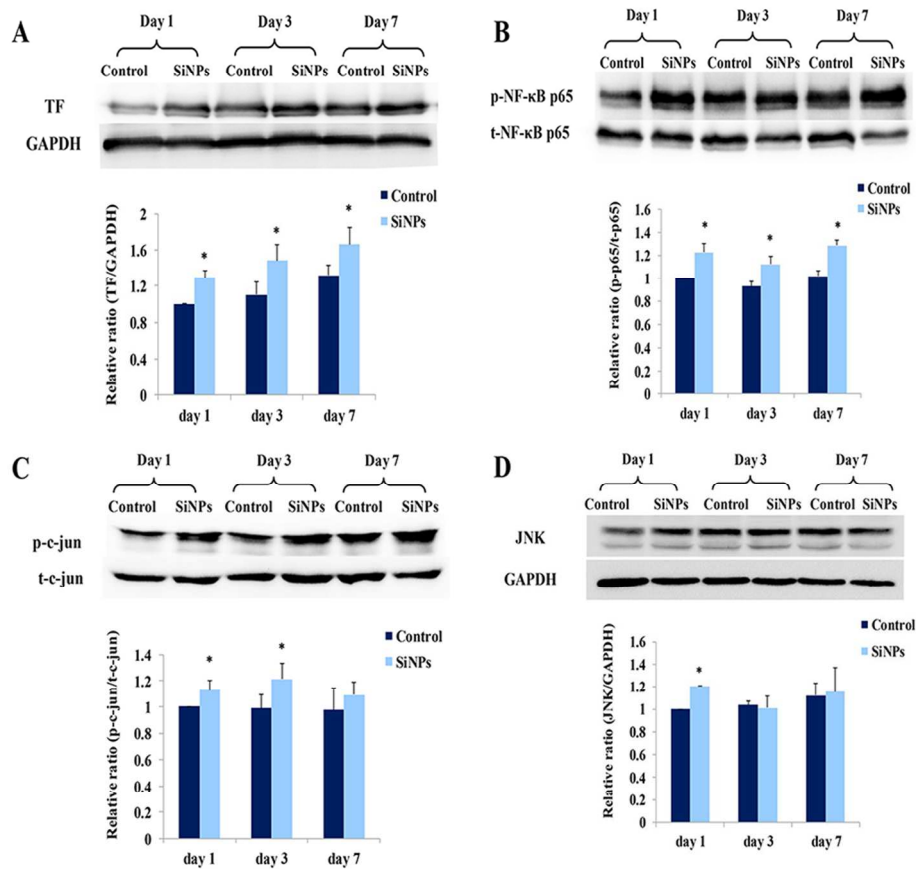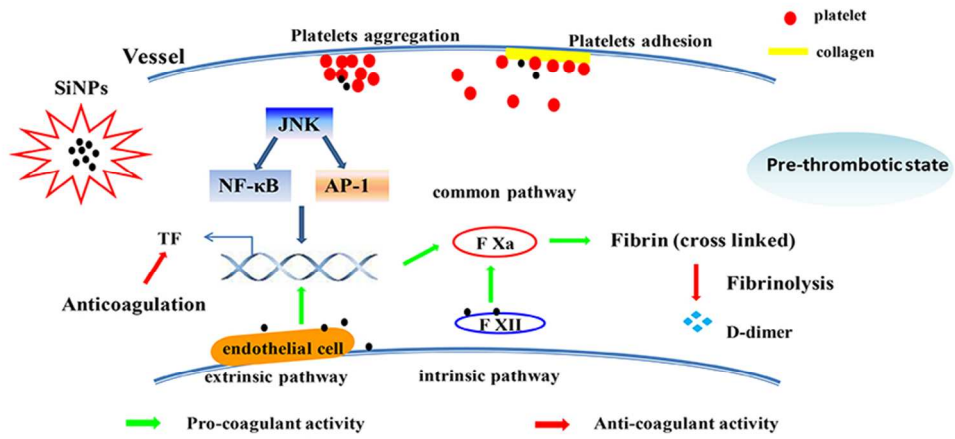153x139mm (300 x 300 DPI)

Figure 9. The molecular mechanism involving in regulating tissue factor (TF) expression in lung tissue after intravenous injection of silica nanoparticles (SiNPs). (A) TF expression; (B) The phosphorylation expression of nuclear factor-κB/p65 (NF-κB/p65); (C) Phosphorylation expression of activator protein-1/ c-Jun (AP-1/c-Jun); (D) The protein levels of c-Jun N-terminal kinase (JNK) measured by Western blot. Data are expressed as mean ± S.D., *$p < 0.05$ vs control group.
170x156mm (300 x 300 DPI)

The pre-thrombotic state induced by SiNPs via interaction between platelets activation, coagulation hyperfunction, anti-coagulation and fibrinolytic resistance.
80x39mm (300 x 300 DPI)